SCULPTING THE KUIPER BELT BY A STELLAR ENCOUNTER: CONSTRAINTS FROM THE OORT CLOUD AND SCATTERED DISK

Harold F. Levison

Department of Space Studies, Southwest Research Institute, Suite 400, 1050 Walnut Street, Boulder, CO 80302; hal@boulder.swri.edu

Alessandro Morbidelli

Observatoire de la Côte d'Azur, B.P. 4229, Boulevard de l'Observatoire, F-06304 Nice Cedex 4, France

AND

Luke Dones

Department of Space Studies, Southwest Research Institute, Suite 400,
1050 Walnut Street, Boulder, CO 80302

ABSTRACT

We investigate the effect that a close stellar encounter would have on the growing scattered disk and Oort cloud. Such an encounter has been suggested by Melita et al. as the cause of the Kuiper belt's outer edge. Thus, we restrict our study to encounters that could have caused such a structure. We find that we probably can rule out all such encounters that occurred either at or subsequent to 10 million years after the Oort cloud started to form. In our simulations, these encounters either produce an extended scattered disk that is too populous to be consistent with observations or produce an Oort cloud that is too anemic.

Key words: comets: general — Oort cloud — solar system: formation — solar system: general

1. INTRODUCTION

Since its discovery in 1992, the Kuiper belt has provided us with an excellent probe for the study of the formation of the outer solar system. The sizes, orbits, and composition of objects in the Kuiper belt supply important clues and constraints for our models of the formation and early dynamical evolution of the giant planets (see Morbidelli & Brown 2004 for a review and Levison & Morbidelli 2003 for some more recent ideas).

In particular, any model of planet formation must explain the very complex structure that is observed. The Kuiper belt is dynamically excited, with many objects having either large inclinations, large eccentricities, or both. And yet, models of the formation of the observed Kuiper belt objects show that these objects must have originally formed in a dynamically cold disk (Stern & Colwell 1997; Kenyon & Luu 1999). These models also show that the original disk in which the observed objects grew should have contained $\sim 10\ M_\oplus$ of material, while there is only $\sim 0.1\ M_\oplus$ currently in the region where these objects are now found (Trujillo & Brown 2001).

Another puzzling characteristic of the Kuiper belt is that there appears to be an abrupt edge to the classical belt near the location of Neptune's 1:2 mean motion resonance at 48 AU (Trujillo & Brown 2001; Allen et al. 2002). Although the exact location of this edge could be the result of the outward migration of Neptune (Levison & Morbidelli 2003), the origin of the edge remains a critical issue. This is due, in part, to the fact that the solution to this mystery may supply clues not only to the formation of the planets, but also to the type of stellar environment in which the solar system formed (Melita et al. 2002; Adams & Laughlin 2001; Hollenbach & Adams 2004).

Indeed, it has been suggested that much of the structure of the Kuiper belt can be explained by a close stellar passage at some time during the early history of the solar system. The effects of a passing star on the Kuiper belt were originally studied by Ida et al. (2000, hereafter ILB00), with a detailed follow-up investigation by Kobayashi & Ida (2001, hereafter KI01). These authors argue that stellar passages were responsible for the dynamical excitation and mass depletion of the primordial Kuiper belt. In addition, Melita et al. (2002) claimed that the Kuiper belt's edge could also result from such an encounter. Although the idea that a passing star is responsible for the dynamical excitation of the Kuiper belt now seems unlikely (Morbidelli & Brown 2004; Gomes et al. 2004), it is still viable for the formation of the Kuiper belt's edge. So, in this paper we concentrate on encounters that might have caused such an edge.

An encounter strong enough to truncate the protoplanetary disk at ~ 50 AU requires that a fairly massive star pass within ~ 200 AU of the Sun. Such an encounter is unlikely to occur in the current Galactic environment (García-Sánchez et al. 1999, 2001). Thus, if one occurred it probably happened while the Sun was in its birth star cluster, where close encounters would have been frequent (Laughlin & Adams 1998; ILB00; Adams & Laughlin 2001; Bate et al. 2003). Figure 1 shows an example of a typical edge-forming encounter. In particular, it shows the orbital element distribution that results from an encounter between an initially dynamically cold Kuiper belt and a star with a mass $M_* = 1\ M_\odot$ and a perihelion distance $q_* = 180$ AU (see § 2 for more detail). The orbit of the perturber also had an inclination with respect to the plane of the Kuiper belt $i_* = 45°$ and an argument of perihelion $\omega_* = 90°$. For its velocity, v_∞, we use the typical relative velocity of stars in star clusters (1 km s^{-1}; Binney & Tremaine 1987). For objects close to the Sun (according to KI01's analytic theory, this means particles with semimajor axes $a \lesssim 0.2 q_*$ in the case of a 1 $M_\odot$ perturber, although this region goes slightly farther out in our calculations) this perturbation has the form of a torque, so that the particle's semimajor axis remains unchanged and the changes in inclination and eccentricity are well behaved [$e \propto (a/q_*)^{5/2}$ and $i \propto (a/q_*)^{3/2}$ according to KI01]. Beyond this critical semimajor axis, the encounter is much more violent, leading to large changes in all the orbital elements of the particles.
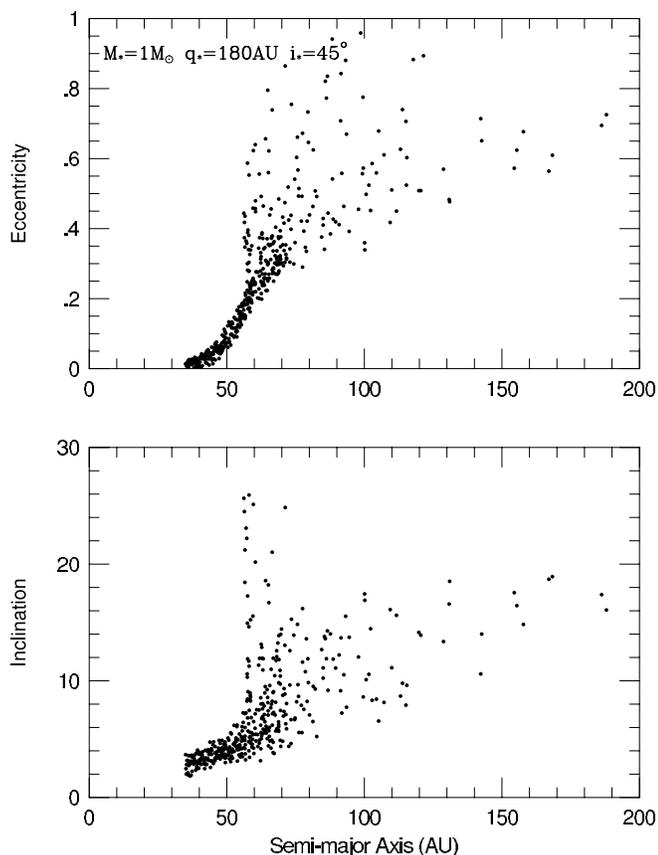
FIG. 1.—Effects of a stellar passage on the Kuiper belt. Objects in the Kuiper belt were initially placed on nearly circular, coplanar orbits between 35 and 100 AU. The figure shows the orbits of the Kuiper belt objects after a 1 $M_\odot$ star passed with a closest approach distance of 180 AU. The orbit of the perturber had an inclination with respect to the plane of the Kuiper belt of $45°$ and an argument of perihelion of $90°$.

One issue that has not been addressed with regard to a close stellar passage is the effect it would have on the Oort cloud. Oort cloud comets are loosely bound to the Sun, and thus small gravitational perturbations could have grave effects on the cloud. This is true because the Sun itself is perturbed. Indeed, we can illustrate this point with a simple calculation. The *impulse approximation* predicts that during a stellar encounter the Sun's velocity will change by $\Delta v \approx 2GM_*/q_* v_\infty$. Plugging in the values for the encounter shown in Figure 1, we find that the Sun will experience a Δv of about 5 km s^{-1}. This value is huge compared with the typical orbital velocity of Oort cloud comets about the Sun, which is roughly 0.2 km s^{-1}.

If the Sun experiences a Δv that is significantly larger than the orbital velocity of the comets, then the Oort cloud will be stripped. Physically what happens is as follows: The Sun and Oort cloud comets are moving through the Galaxy or star cluster as a loosely bound group. When the perturbing star comes by, the Sun's velocity changes by $\sim$5 km s^{-1}. However, since the Oort cloud comets are typically much farther from the star, their velocity change is usually small. Thus, the Sun heads off in a new direction while the bulk of the Oort cloud continues on its original trajectory. And since the Sun's Δv is large compared with the escape velocity of the typical Oort cloud comet, the Sun cannot drag the comets with it and thus the cloud is stripped.

So, can we rule out such an encounter because the Oort cloud exists? No, because the Oort cloud was not always there. Indeed, according to modern models (Duncan et al. 1987; Fernández

1997; Dones et al. 2004), the Oort cloud grew slowly and in stages, taking roughly 10^9 years to fully form. Figure 2 shows the temporal evolution of the Oort cloud in a simulation that assumes the Sun is not in a cluster (we discuss this issue in more detail below). We show the results from Dones et al. (2004, hereafter DLDW04), but these results are characteristic of all modern calculations. In this simulation, massless test particles were initially placed between and slightly beyond the giant planets. During the initial stages of Oort cloud formation, the giant planets scatter objects outward in semimajor axis, making a disklike structure we call the *scattered disk* (see Duncan & Levison 1997). This process occurs fastest for objects initially in the Jupiter-Saturn zone. So, at 10^6 yr most of the objects initially in the Uranus-Neptune zone are still in nearly circular orbits, while those that started in the Jupiter-Saturn region have been scattered outward. As can be seen in Figure 2, at 10^6 yr most members of the scattered disk have perihelion distances less than $\sim$10 AU. Since the planets cannot effectively change a highly eccentric comet's perihelion distance, during this phase a comet's semimajor axis changes (in a random walk), but its perihelion stays in the planetary region (Duncan et al. 1987).

Once a particle reaches $\sim$10,000 AU, the gravitational effects of the Galaxy become important. These effects act as a tide, and thus a particle's perihelion distance can be changed but its semimajor axis remains roughly fixed (see, e.g., Duncan et al. 1987). In this way the Oort cloud is formed. Figure 2 shows that this process is well on its way by 10 Myr; however, at this point in time only 5% of the objects that eventually evolved into the Oort cloud in DLDW04's simulations have yet reached it. By 100 Myr, this fraction is 21%. Note also that the structure of the scattered disk has changed. By this time, Saturn has cleared out most objects crossing its orbit and most of the scattered-disk objects have perihelia outside of 10 AU. By 1 Gyr the scattered disk is mostly depleted—containing only $\sim$5% of the original particles. At this time, the Oort cloud contains 8% of the particles that were originally in the protoplanetary disk. The rest have been ejected to interstellar space.

Since the Oort cloud took so long to form, then perhaps it is possible for a strong stellar encounter to have occurred before the Oort cloud fully formed. If so, we may be able to obtain an interesting constraint on the timing of such an encounter from looking at the effects it has on the Oort cloud and scattered disk. That is the main goal of this paper. In § 2, we present our modeling of our strong stellar encounters and discuss the time constraints. We also discuss our two 4 Gyr simulations. In § 3, we describe the remainder of our simulations. Section 4 contains our conclusions.

2. STRONG STELLAR ENCOUNTERS AND THE LONG-TERM SIMULATIONS

The goal of this section is to determine the effects that a passing star would have had on the forming Oort cloud as a function of the time of the encounter. The first step in this investigation is to find a set of stellar encounters that can be responsible for the edge of the Kuiper belt. We accomplished this by performing a set of direct numerical integrations using the RMVS3 orbit integrator (Levison & Duncan 1994).[1] We start with a disk containing 500 massless test particles on nearly circular, coplanar orbits uniformly distributed about the

---

[1] When we started this project, we were somewhat concerned that RMVS3 would not perform well in a system in which there was a perturber as massive as the Sun. So, we performed a series of tests comparing RMVS3 with a Bulirsch-Stoer integrator and found that RMVS3 performed flawlessly.
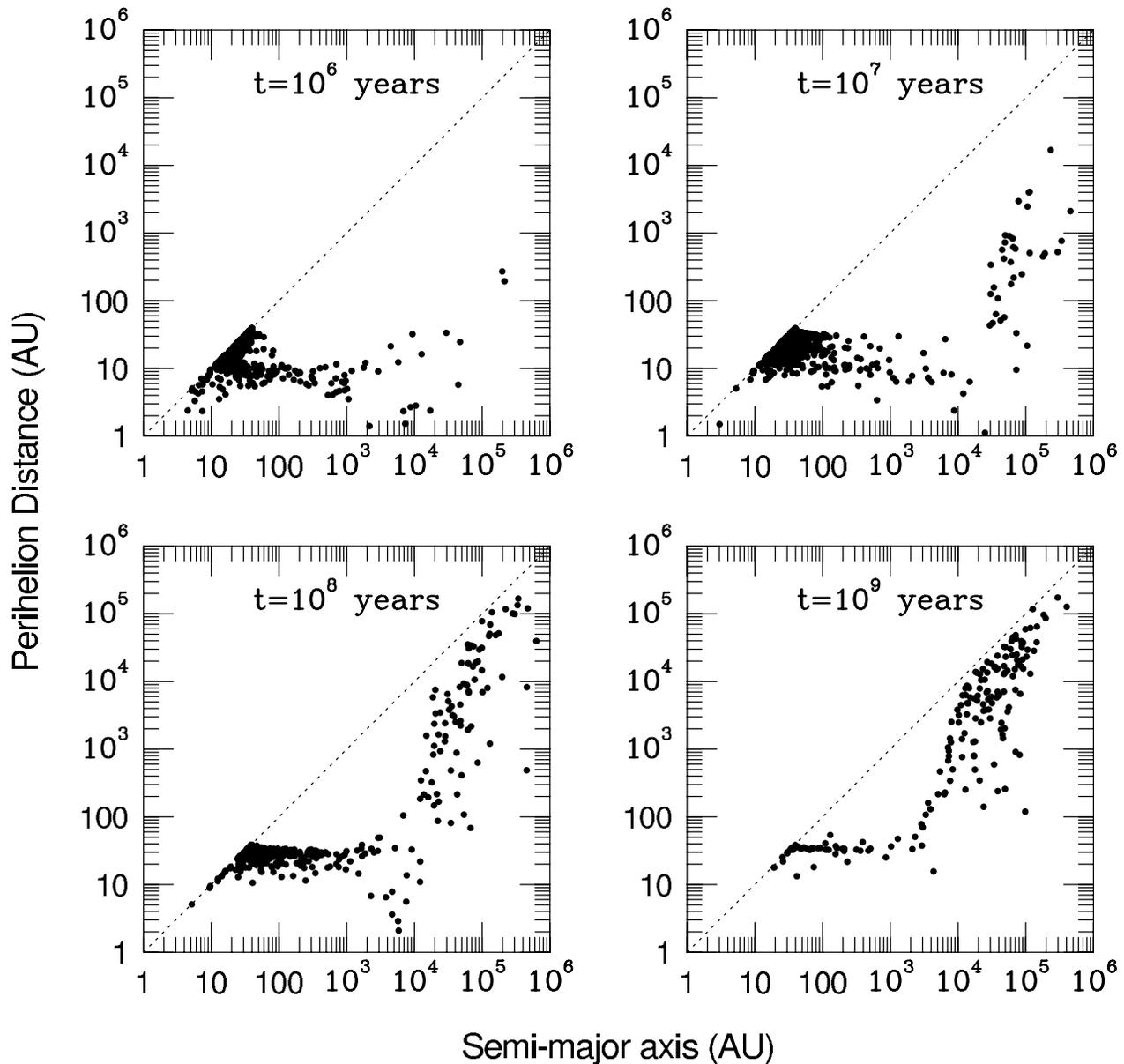
Fig. 2.—Snapshots of the Oort cloud formation model of DLDW04 taken at four different times: 10^6, 10^7, 10^8, and 10^9 yr. Perihelion distance is plotted against semimajor axis. The dotted line shows the location of circular orbits. The region above the dotted line is forbidden.

Sun between 35 and 100 AU. The eccentricities and inclinations (in radians) of the particles were set to 0.01, and the other angles were randomly chosen. The perturbing star was always on a hyperbolic orbit about the Sun, characterized by an encounter speed v_∞, and always had an initial heliocentric distance of 500,000 AU. We varied v_∞, the mass of the star (M_*), its perihelion distance (q_*), its inclination (i_*), and its argument of perihelion (ω_*). The longitude of the ascending node is not an important parameter, because the disk is axisymmetric.

We followed the dynamical evolution of the system containing the Sun, star, and test particles for 6 Myr. In all we performed 27 simulations of various stellar configurations. Our goal was not to uniformly cover parameter space but to find a variety of encounters that significantly excited the Kuiper belt. By "significantly excited" we mean that the median eccentricity (e_{med}) of objects with semimajor axes between 45 and 55 AU was large enough to form an edge either by (1) placing objects on Neptune-crossing orbit, where they will be dynamically removed

($e_{med} \gtrsim 0.4$), or (2) creating relative velocities between the particles large enough to cause a collisional cascade ($e_{med} \gtrsim 0.05$; see § 4 for a detailed discussion). The first case corresponds to an edge-forming event that occurred *after* the formation of the large Kuiper belt objects, while the second case is relevant before the observed objects accreted. Thus, we restrict ourselves to encounters that produce an e_{med} between 0.05 and 0.4 to account for both cases. Figure 1 shows the results of a typical simulation. In this case $M_* = 1\ M_\odot$, $v_\infty = 1$ km s^{-1}, $q_* = 180$ AU, $i_* = 45°$, and $\omega_* = 90°$. These results are consistent with the results of ILB00 and KI01. We found 14 encounters that meet our criteria. They are listed in Table 1.

Our next step was to perform a series of direct numerical integrations of the effect of the stellar encounters shown in Table 1 on the growing Oort cloud at different times. We adopt the simulations of Oort cloud formation by DLDW04 (Fig. 2) as our fiducial, unperturbed case. DLDW04 repeated the study of Duncan et al. (1987), starting with "comets" with semimajor

TABLE 1
Configurations of the Encounters

No.	M_* ($M_\odot$)	q_* (AU)	v_∞ (km s^{-1})	i_* (deg)	ω_* (deg)	e_{med}
Star 1	1	200	10	45	90	0.06
Star 2	1	200	1	45	0	0.06
Star 3	$\frac{1}{10}$	120	1	20	90	0.07
Star 4	1	180	1	45	90	0.08
Star 5	1	125	1	135	0	0.08
Star 6	$\frac{1}{4}$	125	1	45	90	0.09
Star 7	1	200	10	45	0	0.10
Star 8	$\frac{1}{10}$	70	1	135	0	0.12
Star 9	1	180	1	45	0	0.12
Star 10	1	185	1	20	0	0.15
Star 11	$\frac{1}{10}$	100	1	45	0	0.25
Star 12	1	140	1	45	90	0.30
Star 13	1	140	1	45	0	0.37
Star 14	1	140	1	20	0	0.42

axes between 4 and 40 AU and initially small eccentricities and inclinations. These initial conditions are more realistic than the highly eccentric starting orbits assumed by Duncan et al. DLDW04 integrated the orbits of 3000 "comets" for times up to 4 Gyr under the gravitational influence of the Sun, the four giant planets, the Galactic tides, and random passing stars.

The Sun was assumed to reside in its present Galactic environment during the formation of the Oort cloud. The model of the Galaxy included both the "disk" and "radial" components of the Galactic tide. These simulations did not include other perturbers such as molecular clouds, or a possible dense early environment if the Sun formed in a cluster (Gaidos 1995; Fernández 1997). This last condition is in contrast with an implicit assumption in this paper. A stellar passage of the severity that we are studying is only likely to happen if the Sun was embedded in a dense star cluster. We chose the DLDW04 simulations because they are the only ones available to us. We believe that this inconsistency will not strongly affect our results. As we describe in detail below, we use the structure of the scattered disk as our main diagnostic. The objects that mostly affect our diagnostic measure have small enough semimajor axes that they would not be sensitive to whether the solar system was in a cluster or not before the encounter. In either case, the perturbations due to the background environment are simply too weak to affect the orbits of these objects.

DLDW04 performed two sets of runs, with dynamically "cold" and "warm" initial conditions. The "cold" runs included 2000 particles with rms initial eccentricity and inclination to the invariable plane equal to 0.02 and 0.01 radians, respectively. The "warm" runs included 1000 particles with initial rms eccentricity and inclination of 0.2 and 0.1 radians, respectively. The results of the two sets were very similar, so we adopt the "cold" runs here.

Our basic procedure for the 98 simulations presented here was as follows:

1. We extracted the position of planets and particles from the DLDW04 calculations at seven specific times. These times were 10^6, 3×10^6, 6×10^6, 10^7, 10^8, 3×10^8, and 10^9 yr. These systems, some of which are shown in Figure 2, were then used as initial conditions for our simulations. They had between 296 and 959 test particles in them depending on the extraction time.

2. We integrated the orbits of these particles during an encounter with each of the 14 perturbing stars in Table 1. We

accomplished this by performing a set of direct numerical integrations using the RMVS3 orbit integrator. These integrations included the Sun, passing star, test particles, and the four giant planets. The effects of the Galaxy were ignored in this step because the integration times are short. As with the Kuiper belt integrations described above, the star was initially 500,000 AU from the Sun, and we followed the system through the encounter.

3. Finally, we calculated the final configuration of the Oort cloud and scattered disk after 4 Gyr. In the three runs we discuss in this section, we accomplished this using a direct numerical simulation with the techniques employed by DLDW04 (described above). These included the Sun, four giant planets, test particles, and Galactic tides. As we describe in more detail below, because these integrations were computationally time-consuming, we used the results of these three direct integrations to allow us to predict this result in the remaining 95 simulations. These remaining simulations are presented in § 3.

The three runs we followed for 4 Gyr are "star 4" at 10^7 yr, "star 4" at 10^8 yr, and "star 14" at 10^7 yr. We begin our analysis with a detailed description of the results of the first of these. Figure 3 shows the distribution of perihelion distance versus semimajor axis for the simulation of an encounter with star 4 done at $\tau = 10^7$ yr after the beginning of Oort cloud formation (i.e., the initial conditions for this simulation were the extraction from the DLDW04 integration at 10^7 yr). Three different times are shown: (a) immediately before the encounter (i.e., the initial conditions, which are the same as those shown in Fig. 2), (b) immediately after the encounter, and (c) at 4 Gyr. Figure 4 shows a close-up of the same data that emphasizes the evolution of the scattered disk.

Before the encounter, the trans-Neptunian region has the structure that is typical of the DLDW04 models. Objects with $a \gtrsim 20,000$ AU typically have large perihelion distances because the Galactic tides are strong enough in this region to lift their perihelia in 10^7 yr (Fig. 3a). Within $a \sim 20,000$ AU, we find a massive scattered disk with $q < 36$ AU (Fig. 3a).[2] At this

_____

[2] The concentration of points on nearly circular orbits with ~35 AU $\lesssim a \lesssim$ 40 AU are stable Kuiper belt objects that were included in DLDW04's initial conditions. These objects were stable in both DLDW04's integrations and those presented here (see Fig. 4c). They are included in our figures for completeness but are not included in our quantitative analysis.
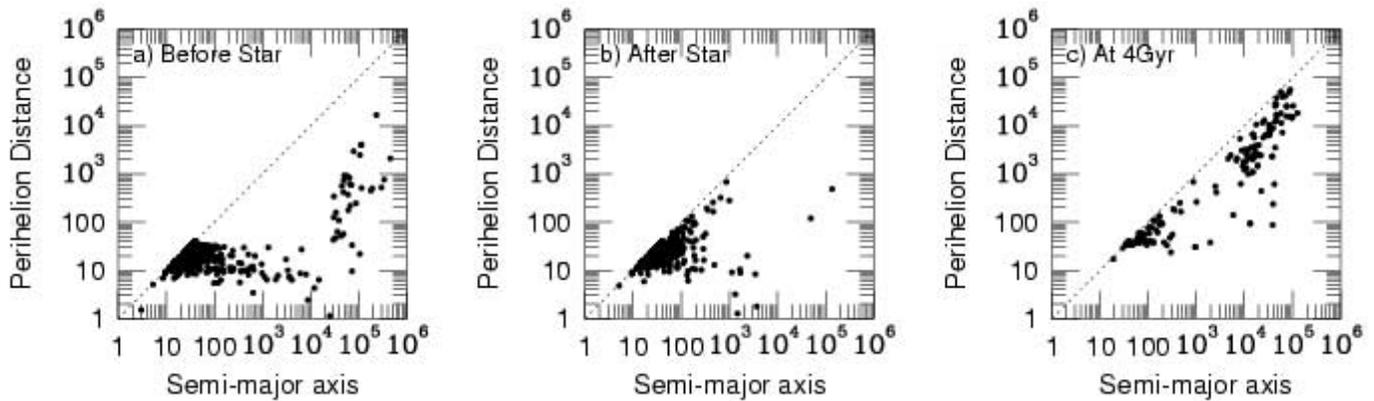
FIG. 3.—The evolution of the Oort cloud in a system in which a star 4 encounter occurs at $t = 10^7$ yr. Perihelion distance is plotted against semimajor axis. The dotted line shows the location of circular orbits. The region above the dotted line is forbidden. (*a*) The *a-q* distribution immediately before the encounter. (*b*) The *a-q* distribution immediately after the encounter. (*c*) The *a-q* distribution at 4 Gyr as determined by a full *N*-body integration.

time, 96% of the particles are in the scattered disk or between the planets. Indeed, 88% of the particles have $a < 100$ AU.

After the encounter, the Oort cloud is stripped (Fig. 3*b*). In particular, 94% of the particles initially with $a > 1000$ AU either are unbound by the encounter or are driven to $q < 10$ AU, where they will be quickly removed by Jupiter and Saturn. However, this does not imply that the solar system would not presently have an Oort cloud if such an encounter had occurred, because 88% of the particles still had $a < 100$ AU. There is still plenty of material left in the system to build an Oort cloud, as can be seen in Figure 3*c*.
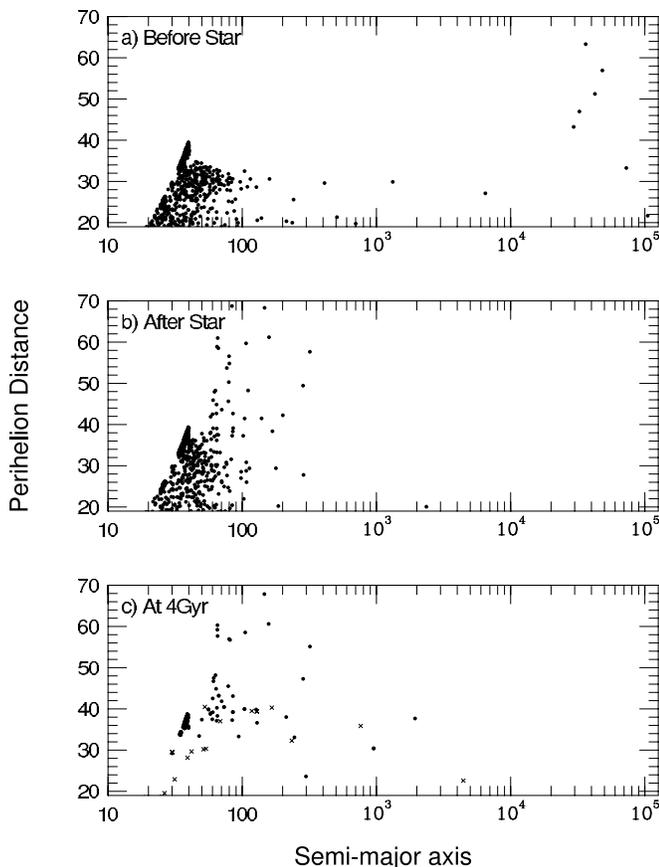

FIG. 4.—Close-up of Fig. 3. The only difference besides scale is in (*c*), where the crosses show the scattered disk predicted by DLDW04 (i.e., the scattered disk if no close encounter occurred).

The real constraint on the early encounter has to do with what happens to the scattered disk. Compare Figures 4*a* and 4*b*, for example. As stated above, before the encounter all scattered-disk objects have $q < 36$ AU. However, after the encounter there is a large population of objects with $a \lesssim 400$ AU and with large perihelion distances. These objects are stable for the age of the solar system, so at 4 Gyr they are still present (Fig. 4*c*, *circles*). Such a population does not exist in the original DLDW04 models (Fig. 4*c*, *crosses*). Thus, this encounter creates a massive "*extended*" (i.e., extended beyond the reach of Neptune) scattered disk (see Gladman et al. 2002 for a discussion of this term).

Indeed, at 4 Gyr we find that there were 61 particles in the scattered disk (50 AU $< a < 1000$ AU). Of these, 19 particles were in the active scattered disk (ASD), which we define as scattered-disk particles with $q < 40$ AU. In addition, 16 particles were in the visible extended scattered disk (VESD), which we are defining as scattered-disk particles with 40 AU $< q < 50$ AU. The remaining scattered-disk objects had $q > 50$ AU. These objects are stable, but present-day surveys are unlikely to discover them. Thus, we ignore them here, although we take this issue up again in a companion paper (Morbidelli & Levison 2004).

Scattered-disk objects with perihelion distances less than 40 AU are not necessarily remnants of the stellar encounter, because they can arise during the normal scattered-disk formation process (Duncan & Levison 1997; Gladman et al. 2002; DLDW04). On the other hand, objects with $q > 50$ AU are faint and thus their detection is challenging. Indeed, the upper limit of 50 AU was chosen because the vast majority of scattered-disk objects have been discovered at heliocentric distances smaller than this. Thus, this model predicts that there should be roughly equal numbers of objects in the ASD and the VESD. Of the 40 scattered-disk objects thus far discovered, only three have $q > 40$ AU (2000 YW$_{134}$ [$a = 58.4$ AU, $q = 41.2$ AU], 1995 TL$_8$ [$a = 52.5$ AU, $q = 40.2$ AU], and 2000 CR$_{105}$ [$a = 230$ AU, $q = 44.4$ AU]).[3]

However, it is not appropriate to compare these two numbers, because the observations suffer from biases while the model does not. In particular, objects with large perihelion distances

_____

[3] As we were about to submit this paper, M. Brown & C. Trujillo announced the discovery of 2003 VB$_{12}$, which has a semimajor axis of 531 AU and an extraordinary perihelion of distance 74.4 AU (Brown et al. 2004). The analysis in this paper does not take this new object into account, but as we explain in footnote 4, we do not believe that this omission affects our results. However, as we explain in our companion paper (Morbidelli & Levison 2004), passing stars probably do play an important role in the history of this object, albeit an encounter that is significantly more distant than the ones studied here.
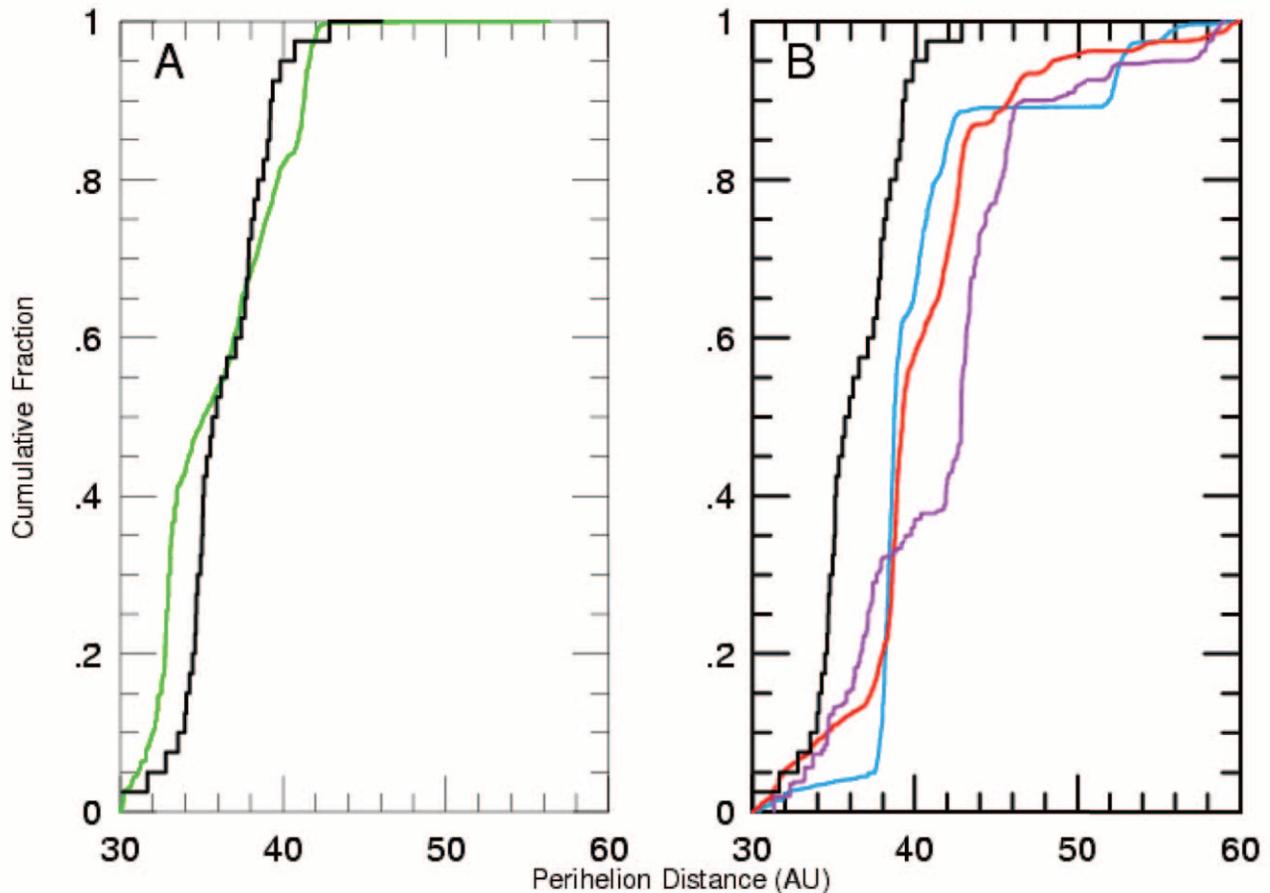
Fig. 5.—Cumulative perihelion distributions. The black curves show the observed distribution of the scattered disk. The green curve is the distribution expected if there were no close stellar encounter. It was calculated from DLDW04's Oort cloud simulations and filtered through our survey simulator (see text). The red, blue, and purple curves show the expected observed distributions for the three 4 Gyr simulations in § 2. These are star 4 at 10^7 yr, star 4 at 10^8 yr, and star 14 at 10^7 yr. While the left panel shows good agreement between the model and observations, the models in the right panel have much larger median perihelion distances than is observed.

are more difficult to see. To correct for this, we need to construct, from our simulations, a model orbital magnitude distribution of the scattered-disk and extended scattered disk populations, convolve it with the observational biases, and compare the results with the observations.

The orbital magnitude distribution model $P(a, q, i, H)$ is constructed by taking the product of an orbital distribution model $p(a, q, i)$ and an absolute magnitude distribution function $N(H)$. For the orbital distribution p, we collected the orbital parameters of the simulated particles over the last 2 Gyr of evolution. Thus, individual particles are included in the distribution many times, but they move around as they dynamically evolve. For the absolute magnitude distribution, we assumed $N(H) \propto 10^{\alpha H}$, where we set $\alpha = 0.7$ according to Morbidelli et al. (2004).

We then biased this orbital magnitude distribution using a method that is a straightforward generalization of that used by Trujillo & Brown (2001). Our implementation is detailed below.

We have taken from the Minor Planet Center the list of the objects with $a > 50$ AU and $q > 25$ AU with multiopposition orbits. From the data reported, we have computed the apparent magnitude and ecliptic latitude of each object at the moment of its discovery, thus obtaining a list of pairs $[V_{\mathrm{disk}}(k), L_{\mathrm{disk}}(k)]$, the index k running over the set of known objects $(1, \ldots, K)$. The way to understand the following procedure is to consider each object as a pointer to a fictitious survey that looked at

magnitude $V_{\mathrm{disk}}(\pm \delta V)$ and at latitude $L_{\mathrm{disk}}(\pm \delta L)$ and found exactly one object. Consider one of these surveys, say, the one corresponding to the kth object. For a set of parameters (a, q, i, H) determined by our dynamical model, we compute the probability $B_k(a, q, i, H)$ that an object with these parameters is discovered by the survey. This is the probability that the object from our dynamical model has apparent magnitude V in the range

$$V_{\mathrm{disk}} - \delta V < V < V_{\mathrm{disk}} + \delta V$$

and latitude L in the range

$$L_{\mathrm{disk}} - \delta L < L < L_{\mathrm{disk}} + \delta L.$$

Therefore, $B_k(a, q, i, H)$ can be easily computed numerically, if one assumes that the values of the angles ω, Ω, and M are random. Now repeat the procedure for all sets of parameters (a, q, i, H) over the region covered by our orbital magnitude distribution model, so that B_k becomes a tabulated function of (a, q, i, H). The function B_k can be considered as the bias function for the survey k. Multiply now the model distribution $P(a, q, i, H)$ by the bias $B_k(a, q, i, H)$, thus obtaining a function $M_k(a, q, i, H)$ that describes the orbital magnitude distribution of the objects that the kth survey could have

discovered. Normalize M_k to unity, so that it becomes a probability distribution.

Now repeat the procedure for all K fictitious surveys. Because each fictitious survey discovered the same number of objects (one each), the overall orbital magnitude distribution of the objects discovered by all surveys is then simply

$$M(a, q, i, H) = \frac{1}{K} \sum_{k=1}^{K} M_k(a, q, i, H).$$

The function M describes the normalized biased distribution of our model.

In order to test the validity of the above procedures (as well as the dynamical models of DLDW04), in Figure 5a we compare the perihelion distance distribution of the observed scattered disk (*black curve*) with that predicted by the combination of the DLDW04 models without a close passing star and our survey simulator (*green curve*). There is relatively good agreement. Indeed, a Kolmogorov-Smirnov (K-S) statistical test (Press et al. 1992), modified as we describe in Appendix A, shows that the probability that the two distributions are derived from the same parent distribution is 0.25.[4] So, we can conclude that our model, without close stellar encounters, is a good representation of the observations.

The red curve in Figure 5b shows the perihelion (q) distribution at 4 Gyr for the scattered disk after the passing star described above (star 4, done at $\tau = 10^7$ yr). This model predicts that 37% of the scattered-disk objects *discovered by observations* should have perihelion distances larger than 40 AU. The modified K-S test (see Appendix A) says that there is less than a 0.1% chance that the observations and this model were derived from the same parent distribution. This stellar encounter produces too many VESD objects and thus can be ruled out.

The blue curve in Figure 5b shows the cumulative q-distribution at 4 Gyr from a simulation of a star 4 passage at 10^8 yr after the Oort cloud started to form. The results are similar to the $\tau = 10^7$ yr simulation and predict that 42% of the detected scattered-disk objects should have $q > 40$ AU, which again is in conflict with the observations. In this case the K-S probability is 2%, which implies that we can rule this model out to better than 2 σ. Finally, the purple curve shows the q-distribution for the star 14 run at $\tau = 10^7$ yr. The modified K-S probability is 0.2%, and thus this model can be ruled out as well.

It should be noted that our simulations did leave out some physical processes that may have been important early in the solar system's evolution—namely, collective gravitational effects and collisions among the disk particles. However, we think that these processes are unlikely to negate the conclusions arrived at in the last paragraph, or described in the next section. These effects are mainly important when considering the response of a high-density, dynamically cold disk to gentle perturbations. Our calculations following the evolution of the scattered disk and Oort cloud are not affected by these processes, because these structures are low-density and excited. These processes could indeed be important when considering

the effect of a stellar passage on the Kuiper belt. However, in this case their main effect will be to minimize the damage that the star can do to the belt. Thus, if we had included these effects in our simulations (which is computationally too expensive to do), we would need encounters stronger than those we are currently studying to form the Kuiper belt's edge. These encounters, in turn, would do even more damage to the scattered disk and Oort cloud. Thus, we believe that if we could include these processes in our calculations, our main results would be strengthened.

3. SHORT-TERM SIMULATIONS

In the last section, we investigated the effect that three stellar passages have on the growing Oort cloud. We showed that according to our models, such encounters would produce a VESD that is more populous than is observed if the encounter occurred at either 10 or 100 Myr after the Oort cloud started to form. In this section we investigate a much wider range of encounters (all the stars in Table 1) at a much wider range of times. As discussed above, there are a total of 95 encounters we wish to investigate.

Unfortunately, we cannot use the methods in § 2, because each simulation described in that section took several CPU-weeks on our cluster of workstations. Performing 95 such simulations is computationally prohibitive. Fortunately, however, the stellar encounters themselves are computationally inexpensive. The difficulty is in following the systems after the encounter to the age of the solar system. Thus, we can study our 95 encounters if we can develop a method to predict the evolution of the system after the encounter from the runs already completed. In particular, we need a method that maps a particle's orbital elements immediately after an encounter to its orbit at 4 Gyr. We develop and test such a map in Appendix B.

We applied the procedures in Appendix B to all of our 98 simulations. Table 2 lists the modified K-S probabilities for these models. These data are also shown in Figure 6. In these simulations, all encounters that occurred at 10^7 yr can be ruled out to better than the $\sim$99% confidence level, while all 10^8 yr encounters can be ruled out to better than the $\sim$94% confidence level. If an encounter occurred during these times, we would see many more objects with $q > 40$ AU than there currently are. We also find that 80% of the 6 Myr encounters can be ruled out to better than 90%. These results (i.e., for times less than 10^8 yr) are independent of the mass of the star.

However, we do see a difference in the behavior of our simulations for times later than 10^8 yr. According to our statistics, we can also rule out encounters of low-mass stars ($\frac{1}{10}$ and $\frac{1}{4} M_{\odot}$) as late as 3×10^8 yr to better than a 97% confidence level. However, the modified K-S probabilities start to increase after 10^8 yr for the 1 $M_{\odot}$ experiments. However, we can probably rule out these late encounters based on the Oort cloud itself. According to DLDW04, the mass in the ASD grows for the first $\sim$10 Myr, at which point it contains roughly 15% of the original protoplanetary disk (minus the mass of Uranus and Neptune), and decreases after that time. By 1 Gyr, for example, the ASD contains only 2% of the available mass. As the number of ASD objects decreases, there are fewer and fewer objects available to build a new Oort cloud if a passing star strips the existing one. So, if a late stellar encounter had occurred we would not have a significant Oort cloud.

We can approximate the mass of the Oort cloud in our simulations using the same techniques employed for calculating $f_{ia, iq}$ (see Appendix B), but here calculating the number of objects we expect in the outer Oort cloud at 4 Gyr. We restrict

---

[4] As described in footnote 3, 2003 VB$_{12}$ was not included in this analysis. When we include it, we find that the modified K-S probability is 0.22, very close to the values quoted in the main text. Thus, we feel justified leaving 2003 VB$_{12}$ out of the remaining analysis in this paper.

TABLE 2
Modified K-S Probabilities for All the Encounters

No.	10^6 yr	3×10^6 yr	6×10^6 yr	10^7 yr	10^8 yr	3×10^8 yr	10^9 yr
Star 1	0.98	0.066	0.049	<0.001	0.001	<0.001	0.016
Star 2	0.41	0.12	0.008	<0.001	0.057	0.002	0.072
Star 3	0.26	0.10	0.060	<0.001	0.001	0.005	0.13
Star 4	0.65	0.055	0.001	<0.001	0.004	0.063	0.11
Star 5	0.39	0.32	0.010	<0.001	0.033	0.015	0.76
Star 6	0.86	0.47	<0.001	<0.001	0.002	0.012	0.70
Star 7	0.90	0.21	0.092	0.004	0.009	0.12	0.28
Star 8	0.23	0.85	0.074	0.001	0.023	0.007	0.56
Star 9	0.46	0.031	0.045	<0.001	0.004	0.012	0.18
Star 10	0.14	0.032	0.027	0.002	0.001	0.12	0.096
Star 11	0.53	0.32	0.036	<0.001	<0.001	0.003	0.097
Star 12	0.49	0.23	0.14	0.002	0.009	0.10	<0.001
Star 13	0.18	0.071	0.015	0.004	0.036	0.043	0.33
Star 14	0.058	0.37	0.28	0.013	0.026	0.27	0.19

ourselves to the outer Oort cloud ($a > 10^4$ AU) because this is the observable region of the cloud (Hills 1981). For the 10^9 yr encounters, we find that we expect between 2.9 and 10.2 particles in the outer Oort cloud. DLDW04 found 59 such particles at 4 Gyr. Thus, Oort clouds in simulations in which a stellar encounter occurred at 10^9 yr will be between ~6 and ~20 times less massive than the Oort cloud would have been if the encounter did not occur, according to our estimates. For the 3×10^8 yr simulations this ratio is between ~3 and ~6.

DLDW04 already find a low efficiency of Oort cloud formation—only ~2.5% of the protoplanetary disk ends up in the outer Oort cloud after 4 Gyr. Assuming an outer Oort cloud population of 5×10^{11} to 1×10^{12} comets (Heisler 1990; Weissman 1996) and an average cometary mass of 4×10^{16} g, DLDW04 predict that the original mass in planetesimals between 4 and 40 AU was ~150–300 $M_\oplus$, some 3–6 times the mass in solids in a "minimum mass" solar nebula. A late stellar encounter would require at least a ~500 $M_\oplus$ disk and probably

more. This amount of mass likely would have produced excessive migration of the giant planets and/or formation of additional giant planets (Hahn & Malhotra 1999; Gomes et al. 2004) and thus can probably be ruled out.

4. CONCLUSIONS

It has been suggested that much of the structure of the Kuiper belt can be explained if the solar system suffered a close encounter with a passing star sometime after the observed Kuiper belt objects formed (Ida et al. 2000; Kobayashi & Ida 2001). The view expressed in these papers is that the observed Kuiper belt objects formed in a quiescent disk that extended beyond the current orbit of Neptune and that this disk was dynamically excited and sculpted by a passing star with a perihelion distance less than ~200 AU. According to these models, the encounter must have happened after the ~10 Myr it takes to build the Kuiper belt objects (Stern & Colwell 1997; Kenyon & Luu 1999; Kenyon & Bromley 2004). In the standard model of planet formation, the stellar passage must therefore have occurred after the Oort cloud and scattered disk started to form.

The purpose of this paper is to ascertain whether either the Oort cloud or scattered disk could place interesting constraints on a stellar encounter like those described above. We performed a series of numerical integrations following the evolution of objects evolving through the scattered disk to the Oort cloud as they are perturbed by a passing star. The characteristics of these stars are listed in Table 1. They were chosen so that they excited objects originally on circular orbits about the Sun at 50 AU to eccentricities between ~0.05 and ~0.4.

According to these models, we find that we can most likely rule out such an encounter at 10 million years and at any subsequent time. Indeed, such an encounter only has a 20% chance of working at 6 million years. For 10^7 yr $\lesssim \tau \lesssim 10^8$ yr (where τ is the time of the encounter), an extended scattered disk is produced in these models that is too populous to be reconciled with observations. If $\tau \gtrsim 10^8$ yr, the Oort cloud would have been too anemic. Thus, we conclude that if the standard model of planet formation is correct, a passing star most likely could not have been responsible for the excitation of the Kuiper belt because we can rule out any encounter that occurred after the time it takes for the observed objects to grow.

It is still possible, however, for a close stellar passage early in the solar system's history to have been responsible for the outer edge of the Kuiper belt (Trujillo & Brown 2001; Allen et al. 2002). Kenyon & Bromley (2002) showed that if a stellar
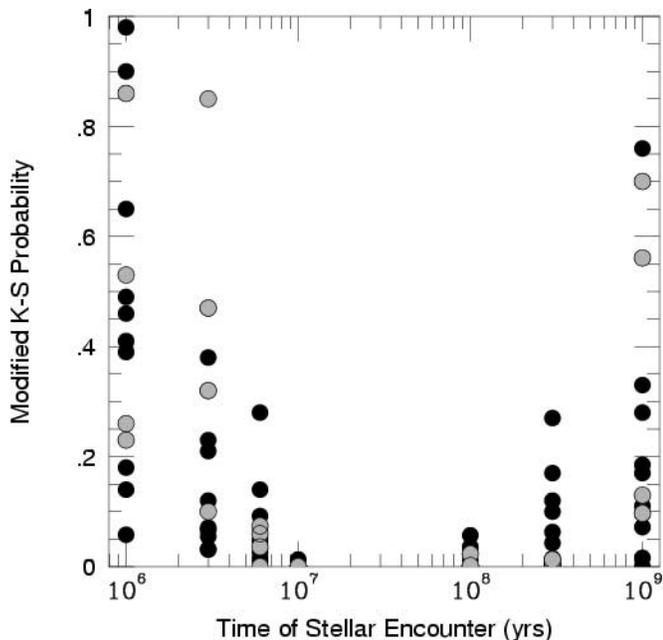

Fig. 6.—Modified K-S probability for all our runs plotted against the time of the stellar encounter. The black circles show the runs with stars of 1 $M_\odot$, while the gray circles show encounters with smaller mass stars.

passage occurred in a disk containing subkilometer icy objects, in the outer regions of the disk, defined to be the region where eccentricities are larger than roughly $e_{crit} = 0.06$, the particles would collisionally grind themselves to dust. However, in the inner regions where $e \lesssim e_{crit}$, collisions would damp out the large eccentricities and inclinations caused by the passing star, and then accretion would continue unabated. Kenyon & Bromley (2002) used these simulations to explain why dust disks around other stars have holes in their central regions. However, we can apply these ideas to the Kuiper belt in order to explain an edge. In particular, if a stellar passage occurred at early times so that the eccentricities at 50 AU (the current visible edge to the Kuiper belt)[5] were equal to e_{crit}, then the region exterior to 50 AU could have suffered a collisional cascade and thus would currently be empty, while normal KBOs still could have formed in the inner regions. Many of the stellar encounters we list in Table 1 excite the disk to this level. So, such a passage would cause an edge to the solar system and could have occurred early in the history of the solar system.

There is an important caveat to the above conclusions. The constraints on the timing of the stellar passage are all with respect to when the Oort cloud and scattered disk started to form. So, an important question is, "When is $t = 0$?" As we stated above, in the standard picture of planet formation these structures start to form along with the planets and thus our conclusions are probably valid.

However, the standard picture of planet formation has not been able to form Uranus and Neptune in their current locations (Lissauer et al. 1995; Levison & Stewart 2001), and it is now widely accepted that Uranus and Neptune could have been transported significant distances after they formed (Fernández & Ip 1984; Hahn & Malhotra 1999; Thommes et al. 1999, 2002; Levison & Morbidelli 2003; Gomes et al. 2004). If the ice giants either formed or, more likely, were transported to their current locations late, as suggested by Wetherill (1975) and Levison et al. (2001), then Oort cloud/scattered disk formation could have been significantly delayed. Indeed, Levison et al. (2001, 2004) argued that the lunar late heavy bombardment (LHB) seen ~3.8 Gyr ago could be observational evidence for such a delay, implying that much of the Oort cloud and Neptune's scattered disk started to form ~700 Myr after solar system formation (the latter defined by the condensation of the first solids).

If there was a significant delay in the formation of the Oort cloud and Neptune's scattered disk, the time constraints that we have set in this paper apply to the time after that delay (e.g., more than ~700 Myr after the solar system formed, for the LHB). This implies that the star could have passed at a much later time relative to solar system formation. However, we think that it is unlikely that a star could have passed through a massive disk between the time at which Neptune formed and the time of the LHB. This is due to the fact that a stellar passage emplaces a lot of disk material on high-eccentricity, Neptune-crossing orbits, which would have triggered Neptune's migration. On the other hand, it is also unlikely that the star passed at ~700 Myr, because close stellar encounters can occur only in dense star-forming regions, which typically disperse on a timescale of a few tens of millions of years (Blitz 1993).

In conclusion, given the above discussion, we believe that it is unlikely that a close stellar encounter occurred after the formation of the large Kuiper belt objects. Thus, the dynamical state of the Kuiper belt cannot be the result of such a passage. If such an encounter is responsible for the formation of the Kuiper belt's edge, the edge probably formed as a result of a collisional cascade as the large Kuiper belt objects were forming.

APPENDIX A

THE MODIFIED K-S TEST

In this paper we use a Kolmogorov-Smirnov statistical test (Press et al. 1992) to determine whether our models are consistent with the data. The K-S test compares two cumulative distributions and calculates the probability that they were drawn from the same parent distribution. It accomplishes this by first calculating a parameter D, which is defined as the maximum absolute value of the difference between the two distributions. Under certain conditions it is possible to calculate a probability distribution (P_D) for D under the assumption that the two populations were indeed from the same parent distribution. If the observed value of D is inconsistent with this probability distribution, we can claim that the two distributions are different.

However, in many situations the analytic function for P_D is not adequate. Unfortunately, we face that problem here. The problem in our case is that the models themselves suffer from small number statistics in a way that the K-S test is not capable of detecting. The problem exists in the models in both §§ 2 and 3, but for different reasons. To get better statistics in § 2, we constructed our distributions by including all the data from the last 2 Gyr of the simulation. Thus, individual particles are included in the distribution many times, but they move around as they dynamically evolve. For the purposes of this discussion, this leads to a model in which the entries are not statistically independent from one another.

A similar thing arises in the models in § 3. In this case we are trying to map a particle distribution immediately after a stellar encounter to one at 4 Gyr. Our procedures include spreading individual particles over a large number of possible orbits. Thus, again we are faced with the situation in which the number of entries in the models is much larger than the actual number of particles that went into calculating that distribution.

Fortunately, Press et al. (1992) supply us with a method of solving this problem: if we cannot use their analytic P_D, we can calculate our own using Monte Carlo techniques. The basic idea is to construct a series of fictitious observed data sets directly from the model. Each of these fictitious data sets contains the same number of entries as the real data set, but they are chosen at random from the model. However, as described above, each entry in our model has a parent particle that it is associated with, and while the number of entries is large, the number of parent particles is small. In order to take the small number of parents into account, when we construct our fictitious data sets, we only include two-thirds of the parent particles.

---

[5] Levison & Morbidelli (2003) argue that the original edge of the proto-planetary disk was at 30 AU and the observed Kuiper belt objects were pushed outward by the migration of Neptune. The exact location of the original outer edge of the disk is not relevant to this argument or the results in this paper.
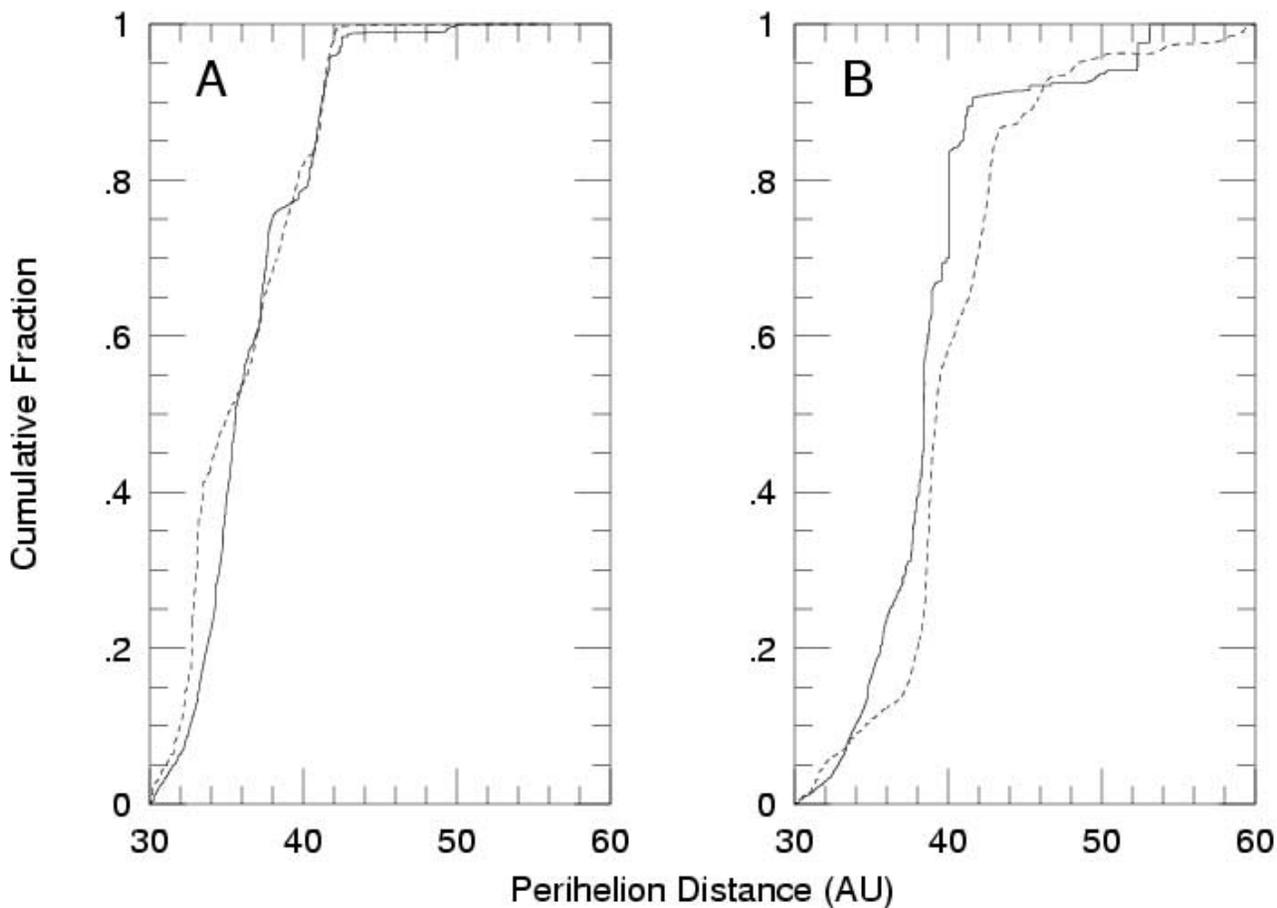
Fɪɢ. 7.—Tests of our prediction methods: the cumulative q-distributions of various models. (a) The dashed and solid curves are derived from DLDW04's Oort cloud simulations and our prediction, respectively. In each case, the model is filtered through our survey simulator (see text). (b) The dashed curve is derived from our full simulation of the star 4 passage at 10^7 yr, while the solid curve shows the results from our predictor.

These are chosen at random and vary from fictitious data set to fictitious data set.

We construct 1000 fictitious data sets. For each we calculate D by comparing it with the full model. Since these fictitious data sets were constructed from the models, the resulting D-distribution should be a good representation of the actual P_D. The modified K-S probabilities described in this paper are simply the fraction of the fictitious data sets that have D's larger than the real data set.

APPENDIX B

PREDICTION MAPPING

As described in § 3, we need a method that maps a particle's orbital elements immediately after an encounter to its orbit at 4 Gyr. The mapping we developed is as follows:

1. We divided the trans-Neptunian region into bins in semimajor-axis and perihelion distance space. We divided semimajor-axis space into four regions: (a) 30 AU $< a <$ 50 AU, (b) 50 AU $< a <$ 100 AU, (c) 100 AU $< a <$ 500 AU, and (d) 500 AU $< a <$ 1000 AU. Perihelion distance is subdivided into bins 2 AU in width. Thus, at any point during our simulations an object can be characterized by an integer pair (ia, iq) describing which bin it is in.

2. Next, for each a-q bin pair we determine the probability that if an object were in that bin immediately after an encounter

it would be in the scattered disk at the end of 4 Gyr. Here by "scattered disk" we mean those objects with 50 AU $< a <$ 1000 AU and 30 AU $< q <$ 60 AU. We make use of the available 4 Gyr simulations to calculate these probabilities or fractions, which we designate as $f_{ia,iq}$. We have several runs to employ for the above purposes. We have the three runs presented in § 2. In addition, we have both the "hot" and "cold" integrations in DLDW04.

3. While $f_{ia,iq}$ can tell us the probability that an object initially in (ia, iq) will be in the scattered disk at the end of the simulation, it does not tell us which orbit it will be in. To accomplish this for each a-q bin, we also keep a list of the orbital elements of scattered-disk objects that resulted from objects originally in it. We define $N_{ia,iq}$ as the number of elements in this list.

This combination of the $f_{ia,iq}$'s and orbital element lists constitutes our map.

For each of the 95 encounters we wish to apply this method to (see § 3), our goal is to develop a scattered-disk distribution from this map. In particular, we develop a list of objects in our final scattered disk, each member of which is assigned a weight (W) that reflects its contribution to the whole. We accomplished this using the following procedures:

1. We extracted the position of planets and particles from the DLDW04 calculations at specific times.

2. We integrated the orbits of these particles during an encounter with one of the perturbing stars in Table 1.

3. We then determined which objects survived the encounter.

4. For each of these particles. we wish to calculate whether it contributes to the final scattered disk and, if so, how much and where. We assigned each of these objects to one of our a-q bin pairs based on its a and q immediately after the encounter. If $f_{ia,iq} \neq 0$, we assume that this particle will eventually end up in one of the orbits in the orbital element list for this bin. Since we do not know which one, we equally distribute this particle to each member of this list. Thus, each member of this list is included in the final scattered-disk model with a weight $W = f_{ia,iq}/N_{ia,iq}$.

5. Finally, we run this distribution through our survey simulator described above.

We can test the above procedure by applying it to situations in which we have complete, 4 Gyr integrations. Figure 7a shows a comparison between the "observed" perihelion distribution of the scattered disk produced by DLDW04's cold run (*dashed curve*) and that predicted by the above procedure (*solid curve*). We generated the solid curve by taking the data from DLDW04's cold run at 10^8 yr (Fig. 2, *bottom left*) and running it through our procedure without a passing star. Another such test can be found in Figure 7b, where the dashed curve is the "observed" scattered-disk q-distribution produced by the passage of star 4 at 10^7 yr as determined in § 2 (same as the blue curve in Fig. 5), while the solid curve shows this distribution predicted by our map. As can be seen, the map reproduces the direct integrations fairly well.

REFERENCES

Adams, F. C., & Laughlin, G. 2001, Icarus, 150, 151
Allen, R. L., Bernstein, G. M., & Malhotra, R. 2002, AJ, 124, 2949
Bate, M. R., Bonnell, I. A., & Bromm, V. 2003, MNRAS, 339, 577
Binney, J., & Tremaine, S. 1987, Galactic Dynamics (Princeton: Princeton Univ. Press)
Blitz, L. 1993, in Protostars and Planets III, ed. E. H. Levy & J. I. Lunine (Tucson: Univ. Arizona Press), 125
Brown, M. E., Trujillo, C., & Rabinowitz, D. 2004, ApJL, submitted (astro-ph/0404456)
Dones, L., Levison, H. F., Duncan, M. J., & Weissman, P. R. 2004, Icarus, submitted (DLDW04)
Duncan, M., Quinn, T., & Tremaine, S. 1987, AJ, 94, 1330
Duncan, M. J., & Levison, H. F. 1997, Science, 276, 1670
Fernández, J. A. 1997, Icarus, 129, 106
Fernández, J. A., & Ip, W.-H. 1984, Icarus, 58, 109
Gaidos, E. J. 1995, Icarus, 114, 258
García-Sánchez, J., Preston, R. A., Jones, D. L., Weissman, P. R., Lestrade, J.-F., Latham, D. W., & Stefanik, R. P. 1999, AJ, 117, 1042 (erratum 118, 600)
García-Sánchez, J., Weissman, P. R., Preston, R. A., Jones, D. L., Lestrade, J.-F., Latham, D. W., Stefanik, R. P., & Paredes, J. M. 2001, A&A, 379, 634
Gladman, B., Holman, M., Grav, T., Kavelaars, J. J., Nicholson, P., Aksnes, K., & Petit, J.-M. 2002, Icarus, 157, 269
Gomes, R. S., Morbidelli, A., & Levison, H. F. 2004, Icarus, 170, 492
Hahn, J. M., & Malhotra, R. 1999, AJ, 117, 3041
Heisler, J. 1990, Icarus, 88, 104
Hills, J. G. 1981, AJ, 86, 1730
Hollenbach, D., & Adams, F. C. 2004, in ASP Conf. Ser. 324, Debris Disks and the Formation of Planets, ed. L. J. Caroff & D. Backman (San Francisco: ASP), in press
Ida, S., Larwood, J., & Burkert, A. 2000, ApJ, 528, 351 (ILB00)
Kenyon, S. J., & Bromley, B. C. 2002, AJ, 123, 1757

Kenyon, S. J., & Bromley, B. C. 2004, AJ, 127, 513
Kenyon, S. J., & Luu, J. X. 1999, ApJ, 526, 465
Kobayashi, H., & Ida, S. 2001, Icarus, 153, 416 (KI01)
Laughlin, G., & Adams, F. C. 1998, ApJ, 508, L171
Levison, H. F., Dones, L., Chapman, C. R., Stern, S. A., Duncan, M. J., & Zahnle, K. 2001, Icarus, 151, 286
Levison, H. F., & Duncan, M. J. 1994, Icarus, 108, 18
Levison, H. F., & Morbidelli, A. 2003, Nature, 426, 419
Levison, H. F., & Stewart, G. R. 2001, Icarus, 153, 224
Levison, H. F., Thommes, E., Duncan, M. J., & Dones, L. 2004, in ASP Conf. Ser. 324, Debris Disks and the Formation of Planets, ed. L. J. Caroff & D. Backman (ASP), in press
Lissauer, J. J., Pollack, J. B., Wetherill, G. W., & Stevenson, D. J. 1995, in Neptune and Triton, ed. D. P. Cruikshank (Tucson: Univ. Arizona Press), 37
Melita, M. D., Larwood, J., Collander-Brown, S., Fitzsimmons, A., Williams, I. P., & Brunini A. 2002, in Asteroids, Comets, Meteors: ACM 2002, ed. B. Warmbein (ESA SP-500) (Noordwijk: ESA), 305
Morbidelli, A., & Brown, M. E. 2004, in Comets II, ed. M. C. Festou, H. U. Keller, & H. A. Weaver (Tucson: Univ. Arizona Press), in press
Morbidelli A., Emel'yanenko, V. V., & Levison, H. F. 2004, MNRAS, in press
Morbidelli, A., & Levison, H. F. 2004, AJ, 128, 2564
Press, W. H., Teukolsky, S. A., Vetterling, W. T., & Flannery B. P. 1992, Numerical Recipes in FORTRAN (2nd ed.; Cambridge: Cambridge Univ. Press)
Stern, S. A., & Colwell, J. E. 1997, ApJ, 490, 879
Thommes, E. W., Duncan, M. J., & Levison, H. F. 1999, Nature, 402, 635
———. 2002, AJ, 123, 2862
Trujillo, C. A., & Brown, M. E. 2001, ApJ, 554, L95
Weissman, P. R. 1996, in ASP Conf. Ser. 107, Completing the Inventory of the Solar System, ed. T. W. Rettig & J. M. Hahn (San Francisco: ASP), 265
Wetherill, G. W. 1975, in Proc. 6th Lunar Science Conference, ed. R. B. Merrill (New York: Pergamon), 1539